Z. Phys. A – Atomic Nuclei 328, 239–245 (1987)

Zeitschrift für Physik A
Atomic Nuclei

K^- – Proton Atomic Transitions*

P.B. Siegel**
Institut für Theoretische Physik, Universität Regensburg,
Federal Republic of Germany

Received March 31, 1987; revised version July 2, 1987

The relation between the $K^- - P$ scattering length and the X-ray spectrum for the $2p \to 1s$ electromagnetic transition in $K^- - P$ atoms is examined. A coupled-channel potential model is used to explicitly calculate the energy of the S-matrix pole in the $1s$ channel, which is then compared with the energy obtained from the scattering lengths via the standard equation. The X-ray spectrum is calculated and compared with the Lorentzian shape associated with the complex energy of the S-matrix pole. In addition, the $K^- p$ branching ratios are compared at threshold and at the complex S-matrix pole energy.

PACS: 36.10.Gv

1. Introduction

There are two ways of determining the $K^- - P$ scattering length: by an analysis of the low energy $K^- - P$ scattering data and from the shift and width of the $1s$ $K^- - P$ atomic level. The values obtained by these methods differ dramatically. A recent analysis of the low energy data by Martin [1] which satisfies dispersion relation constraints gives values of $a_0 = (-1.70 + 0.68i)$ fm and $a_1 = (0.37 + 0.60i)$ fm for the isospin 0 and 1 $K - N$ scattering lengths. Using these values in (1) below, which relates the scattering length to the atomic level shift, ε, and width, Γ, one obtains a value of $\varepsilon - i\frac{\Gamma}{2}$ equal to $+407 - 263i$ eV. Other analyses [2] of the scattering data give similar results: the atomic level shift ε should be positive and between 200–400 eV. The $K^- - P$ system is complicated by the presence of a resonance, $\Lambda(1405)$, close to the $K^- - P$ threshold energy, and the scattering data analyses include this feature. However, the existing experimental data for the $K^- - P$ atom show a negative $1s$ energy level shift. Three measurements have been performed with values for (ε, Γ) in eV of $\left(-40 \pm 60, 0\,^{+230}_{-0}\right)$ [3], $(-270 \pm 80, -560 \pm 260)$ [4], and $\left(-190 \pm 60, 80\,^{+200}_{-80}\right)$ [5]. This discrepancy has been discussed with respect to the nature of the $\Lambda(1405)$ resonance [6] and, also, the possibility of an anomalously large Coulomb effect [7]. These suggestions, however, are unable to clearly reconcile the problem [8, 9]. In this paper we examine the range of validity of (1) when a bound state resonance is near threshold, and estimate how much the X-ray spectrum is shifted from this energy.

The relationship between the scattering length and the $1s$ atomic level shift, ε, and width, Γ, for the $K^- - P$ atom is approximately given by [10]

$$\varepsilon - i\frac{\Gamma}{2} = -412\, a_c(\text{eV/fm})$$

where

$$a_c = \left\{ \frac{1 + |k_0|(a_0 + a_1)/2}{|k_0|\, a_0\, a_1 + (a_0 + a_1)/2} + \frac{2}{B}\left(2\gamma + \ln\left(\frac{2d}{B}\right)\right) \right\}^{-1}. \quad (1)$$

Here B is the Bohr radius, γ is Euler's constant, and k_0 is the momentum of the virtual $K^0 - n$ state. The

* Work supported in part by Deutsche Forschungsgemeinschaft (grant We 655/9-1)
** Present Address: California State Polytechnic University Pomona

parameter d is a cutoff radius and taken to be 0.4 fm [10]. The scattering lengths a_0 and a_1 correspond to the isospin $I=0$ and 1 scattering lengths respectively assuming $[H, I]=0$. The above relationship derives from the scattering length approximation when the S matrix is analytically continued below the $K^- - P$ threshold. Isospin breaking and simple Coulomb corrections are taken into account. The complex energy $\varepsilon - i\frac{\Gamma}{2}$ is the difference between the s-wave pole of the S matrix with $\left(E_p - i\frac{\Gamma}{2}\right)$ and without (E^c_{1s}) the hadronic interaction:

$$\varepsilon - i\frac{\Gamma}{2} = (E_p - E^c_{1s}) - i\frac{\Gamma}{2}. \tag{2}$$

In Sect. 3, we explicitly calculate the pole energy and compare the results with the predictions of (1).

Since the pole energy is complex, it is not what is measured in a $2p-1s$ electromagnetic transition. One measures instead an energy spectrum for the emitted X-ray, $X(E)$, whose peak value is at an energy which we label here as E_0. When Γ/E_0 is very small, the spectrum is almost exactly Lorentzian and can be described by two parameters. As the inelasticity increases, then the spectrum begins to deviate from a pure Lorentzian shape and the peak position can shift. Due to the presence of the $\Lambda(1405)$ resonance near the $K^- - P$ threshold, the $1s$ level for this system may have a large width. In Sect. 3, we estimate the deviations to the center position and Lorentzian shape for this system. The determining factor for these modifications is the ratio Γ/E_0. As we shall see, when Γ/E_0 is as large as 0.1, the energy difference between the $2p$ atomic state, E^c_{2p}, and E_p can be quite different from E_0. We treat the problem in a time independent manner and assume that the interaction can be represented by potentials between the various channels. The details of this coupled-channel potential model are described in the next section.

2. The Coupled Channel Calculation

We carry out the calculation in coordinate space, since numerically it is easier to include the Coulomb potential in this representation. The effective channels are $\Sigma^+\pi^-$, $\Sigma^0\pi^0$, $\Sigma^-\pi^+$, $\Lambda\pi^0$, K^-p, K^0n, and are labelled 1–6 respectively. The set of coupled differential equations which describes the system is given by

$$k_i^2(E)\,\Psi_i = -\nabla^2\,\Psi_i + 2\mu_i \sum_j V_{ij}\,\Psi_i + V^i_{\text{Coulomb}}\,\Psi_i \tag{3}$$

where

$$k_i^2(E) = (E^2 - (m_B^i + m_m^i)^2)(E^2 - (m_B^i - M_m^i)^2)/4E^2$$

and the reduced energy of the meson-baryon system is

$$\mu_i(E) = \frac{\sqrt{m_B^{i2} + k_i^2}\,\sqrt{m_m^{i2} + k_i^2}}{\sqrt{m_B^{i2} + k_i^2} + \sqrt{m_m^{i2} + k_i^2}}.$$

Here, the baryon and meson masses are labeled m_B^i and m_m^i respectively for channel i. Limiting the analysis to s-wave and defining u_i as $r\psi_i$, Eq. (3) becomes

$$k_i^2\,u_i = -\frac{d^2u_i}{dr^2} + 2\mu_i(E)\sum_j V_{ij}\,u_i + V^i_{\text{Coulomb}}\,u_i. \tag{4}$$

V^i_{Coulomb} is a point Coulomb potential for the Σ-π charged channels and is taken to be the potential of a uniformly charged sphere of radius .8 fm for the $K^- - P$ system. Results are insensitive to the choice of this radius. We are interested in two calculations, each requiring different sets of boundary conditions. First, we evaluate the pole of the S matrix. In the second calculation, the matrix element for the electromagnetic transition from the $2p$ to the $1s$ level is evaluated as a function of energy.

For determining the pole of the scattering matrix we search for the energy $E_p - i\frac{\Gamma}{2}$ for which $u_i(0)$ vanishes and $u(r)$ has the asymptotic forms for large r of e^{ik_ir} for the uncharged channels and the corresponding Coulomb functions for the charged ones. For channels 5 and 6, which are below threshold, $im(k)$ is greater than zero and the wave function goes to zero for large r. For channels 1–4, which are scattering states, $im\,k$ is negative and $u_i(r)$ diverges for large r. These coordinate space boundary conditions quantize the complex energies, whose $1s$ value is given approximately by (1) if the effective range expansion is valid and simple Coulomb corrections suffice. We compare this eigenenergy with the predictions of (1) in the next section.

Similar calculations of this type have recently been performed by Thaler [11] and Landau and Cheng [12] for specific potential models which fit the scattering data. Here we examine more specifically the general validity of (1). Also, our approach is different in some respects. The coupled-channel equations are solved in coordinate space, instead of a momentum basis. This allows a straightforward inclusion of the Coulomb interaction, as well as simpler numerics for obtaining an accurate solution. For the local potential, all six channels are easily included instead of using a complex potential to incorporate the $\Lambda\pi$ channel. We are able, therefore, to investigate the K^-p

threshold branching ratios. In addition, in the present work the electromagnetic transition matrix element, discussed next, is explicitly calculated. Other corrections to (1) have also been considered [13], but these can be model dependent and are usually small. We focus our attention here on the Dalitz-Tuan formula, Eq. (1) since it is often referred to, is simple to apply and as we shall see is generally accurate.

Since the process is purely electromagnetic, we assume that the transition is from one $K^- - P$ state to another. The electromagnetic dipole transition rate between the $2p$ and $1s$ atomic level is given by:

$$w = \frac{4e^2}{3\hbar^4 c^3} q_\gamma^3 |\langle \Psi_f | r | \Psi_i \rangle|^2 \tag{5}$$

where q_γ is the energy of the emitted X-ray.

For the $K^- - P$ atom, the initial wave function ψ_i can be well approximated by the time independent $2p$ atomic wave function without hadronic couplings, ψ^c_{2p}, since the width of this level is very narrow. The final state ψ_f, however, is time dependent and can have a large width. This state decays via the strong interaction into the free Σ-π and Λ-π channels. We assume that the spatial representation $u_5(E, r)$ for a given real energy E of this $1s$ state is a solution of (4), and subject to the conditions

$$u_5(E, 0) = 0; \quad \lim_{r \to \infty} u_5(E, r) = 0; \tag{6}$$

and

$$\int_{E_1}^{E_2} \int_0^\infty |u_5(E, r)|^2 \, dr \, dE = 1,$$

where the limits of integration are broad enough to include all contributions of the resonance. The incoming boundary conditions for the free $\Sigma\pi$ and $\Lambda\pi$ channels are not changed with energy. One particular choice of these could be for instance an incoming wave only in channel i. The outgoing waves of the free $\Sigma\pi$ and $\lambda\pi$ channels will, of course, depend on the energy. Note, u_5 has the units of (distance $\times$ energy)$^{-1/2}$. With this energy dependent wave function, one can calculate an energy dependent transition rate $W(E)$, such that $W(E)\,dE$ represents the probability for an X-ray to be emitted between the energy E and $E + dE$:

$$W(E)\,dE \equiv \frac{4e^2}{3\hbar^4 c^3} q_\gamma^3(E) |\langle \Psi_5(E) | r | \Psi_{2p} \rangle|^2 \, dE \tag{7}$$

where

$$q_\gamma(E) = E_{2p} - E$$

and

$$\Psi_5(E, r) = \frac{u_5(E, r)}{r}.$$

If $W(E)$ does not depend strongly on the free-channel incoming boundary conditions, then it is to be compared with the experimentally observed X-ray spectrum $X(E)$.

Consider the radial and energy dependence of the state $u_5(E, r)$ defined by the conditions of (6). For r greater than the range of the strong interaction R_s, the channel couplings vanish. In this region the wave function $u_5(E, r)$ is proportional to the Wittaker function of the second kind which we label here as $W_2(E, r)$. For r smaller than R_s, the precise nature of $u_5(E, r)$ depends on the wave functions of the free channels, u_{1-4}, which in turn depend on their incoming boundary conditions. However, since R_s is much smaller than the Bohr radius B, these interactions modify only a small fraction of $u_5(E, r)$. The matrix element in (7) is very insensitive to the values of ψ at these comparatively small distances. The corrections are of order $(R_s/B)^3$. The incoming boundary conditions essentially only determine the overall scale of this matrix element. The absolute magnitude of $W(E)$ is determined from the normalization requirement in (6).

The energy dependence of $u_5(E, r)$ is governed primarily by the pole of the S matrix. Thus, u_5 is approximately given by

$$u_5(E, r) \approx \frac{N}{E - \left(E_p - i\frac{\Gamma}{2}\right)} W_2(E, r), \tag{8}$$

if the incoming boundary conditions for the free channels, on which the overall normalization depends, are not changed with energy. For an initial incoming wave in channel i, N_2 is proportional to the partial decay width, Γ_i, of this channel. Thus to a very good approximation, the shape of the function $W(E)$ is independent of the choice of the incoming boundary conditions of the free channels. If R_S would be of the same order as B, the function $W(E)$ would depend on these boundary conditions, the inelasticity would be large and the time-independent approximation method employed here would not be valid. For all cases considered in this paper, the shape of $W(E)$ did not vary more than 1% for different choices of boundary conditions.

In the limit of weak coupling, Γ/E_p is much less than 1, and $u_5(E, r)$ is approximately given by

$$u_5 k(E, r) \approx \frac{\sqrt{\Gamma/2\pi}}{E - \left(E_p - i\frac{\Gamma}{2}\right)} r \Psi^c_{1s}(r) \tag{9}$$

Table 1. Comparison of the atomic level shift ε and width Γ as calculated from (1), from the pole of the S matrix, and from the peak and width of the transition rate $W(E)$. The range of the potential is $\alpha = 500$ MeV

$f^2/4\pi$	a_0(fm)	a_1(fm)	Eq. (1) (ε, $\Gamma/2$) eV	S-matrix Pole (ε, $\Gamma/2$) eV	$W(E)$ (ε, $\Gamma/2$) eV
0.6	1.51 +0.44i	0.24+0.07i	(−344, 95)	(−353, 100)	(−354, 100)
0.7	2.23 +1.97i	0.31+0.11i	(−515, 314)	(−533, 380)	(−542, 390)
0.8	−0.41 +3.6i	0.39+0.18i	(−206, 848)	(−104, 869)	(−157, 870)
0.82	−0.91 +3.2i	0.40+0.20i	(− 59, 845)	(+ 41, 828)	(− 10, 830)
0.84	−1.20 +2.8i	0.42+0.22i	(+ 61, 796)	(+143, 752)	(+100, 750)
0.9	−1.35 +1.84i	0.46+0.29i	(+216, 579)	(+244, 526)	(+222, 530)
1.0	−1.109+1.14i	0.53+0.47i	(+198, 387)	(+199, 355)	(+189, 360)

where $\psi^c_{1s}(r)$ is the normalized time independent Coulomb $1s$ atomic wave function. The transition probability $W(E)$ becomes

$$W(E) \simeq \frac{2e^2 \Gamma q_\gamma^3(E)}{3\pi\hbar^4 c^3 \left[(E-E_p)^2 + \frac{\Gamma^2}{4}\right]} |\langle \Psi^c_{1s}|r|\, \Psi^c_{2p}\rangle|^2 \qquad (10)$$

with the characteristic Lorentzian shape. As the inelasticity increases, $W(E)$ begins to differ from a pure Lorentzian centered about E_p. This deviation is caused by the phase space factor $q_\gamma(E)$, which favors larger values of E, and the energy dependence of the shape of the wave function. For higher energies, $\psi_5(E, r)$ peaks at larger r, and the transition integral which contains the factor r^3 is bigger than for wave functions of a lower energy.This latter property favors smaller values of E. As shown in Table 1, when Γ/E_p is of the order of 0.1 the maximum of $W(E)$ can be shifted significantly from E_p. In the next section we investigate, for a particular model of the $K-N$ system, the importance of these modifications.

3. Results

We first consider the validity of (1). For this evaluation, we choose two alternative potential forms, local and non-local, which give qualitative agreement with the above threshold scattering data. For the local potentials, a Yukawa form

$$V_{ij}(r) = C_{ij} \frac{f^2}{4\pi} \frac{e^{-\alpha r}}{r} \qquad (11)$$

is used, where the C_{ij} coefficients are determined from $SU(3)$ symmetry assuming vector meson exchange between the baryon and the pseudoscalar meson octets. This same potential is used in Ref. 14. For the non-local potentials we choose the simple separable form

$$V_{ij}(k, k') = C_{ij} f^2 \left(\frac{\alpha}{\alpha^2 + k^2}\right)\left(\frac{\alpha}{\alpha^2 + k'^2}\right) \qquad (12)$$

with the same relative coupling, C_{ij}, between the channels. For a given strength f^2 and range α, we calculate the scattering lengths and determine the pole position from (1). This value is then compared to that obtained by solving the coupled channel equations for the actual pole using the method of the previous section.

The above potentials give a fair description of the low energy scattering data and therefore suffice for our purpose of examining the validity of (1). Although there are two parameters, the pertinent factor for the scattering length is the ratio f^2/α. This can be understood considering the single channel problem for a potential of the form $\alpha f^2 V(\alpha r)$ where f^2 is a dimensionless strength. Rescaling the momenta in units of the range, we have

$$k'^2 u = -\frac{d^2 u}{dx^2} + 2\frac{\mu f^2}{\alpha} V(x) \qquad (13)$$

where x equals αr and k' equals k_5/α. The low energy hadronic phase shift has the functional form $\delta_0 = k' A(f^2 \mu/\alpha)$, and the scattering length is given by

$$a = \lim_{k \to 0} \frac{ki' A(f^2 \mu/\alpha)}{k} = \frac{1}{\alpha} A(f^2 \mu/\alpha) \qquad (14)$$

where the function $A(f^2 \mu/\alpha)$ depends on the potential. For the full coupled channel problem, A will have some dependence on the momenta of the other channels at the $K^- - P$ threshold energy, and (14) is only approximate. This dependence is not strong, and one obtains similar results using a different range and a potential strength roughly scaled as $f'^2 = f^2 \frac{\alpha'}{\alpha}$. To get a feeling for the appropriate magnitudes, we note,

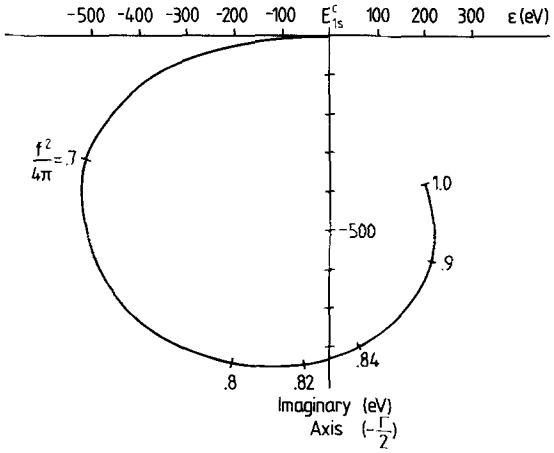

Fig. 1. Plot of the pole of the S matrix in the complex plane associated with the $1s$ $K^- - P$ atomic level as a function of hadronic coupling strength. The numbers alongside the curve refer to values of the potential strength parameter $f^2/4\pi$. The range of the potential is fixed at $\alpha = 500$ MeV

that for a range of 800 MeV, roughly the mass of a vector meson, a value for $f^2/4\pi$ of 1.34 produced a bound state resonance at 1405 MeV with a width of 25 MeV. In a simple vector meson exchange model of the $K^- p$ amplitude, the corresponding ρNN coupling strength is $g^{v^2}_{\rho NN}/(4\pi) = 0.55$ (using $g^T/g^V = 6$ and $g_{\rho KK} = g_{\rho\pi\pi}/2 = 3.0$), which is comparable with the values of 0.25 – 0.8 listed in Table 9.2 of Ref. 15. Our analysis included values of 200 – 1000 MeV for the range parameter α.

Results for the local potential with $\alpha = 500$ MeV are shown in Fig. 1. We chart the movement of the pole in the complex plane as a function of the overall potential strength $f^2/4\pi$. This locus is easily understood: The pole starts at the unshifted energy E^c_{1s} for $f^2 = 0$, and is initially lowered in energy ($\mathrm{Re}(\varepsilon) < 0$) due to the attraction of the strong potential. As f^2 is increased further, greater inelasticity sets in and the trail veers downward (larger Γ). Eventually, an unstable quasi-bound state is formed and the pole turns back. When this resonance is near threshold ($f^2/4\pi \sim 0.82$), Γ is maximized and $\mathrm{Re}(\varepsilon)$ starts becoming positive, a consequence related to Levinson's Theorem. Continued increase of the potential strength lowers the resonance below threshold, the inelasticity decreases, and $\mathrm{Re}(\varepsilon)$ becomes more positive. This resonance is moved down to 1405 MeV for $f^2/4\pi = 0.91$. Smaller (larger) values of α will continuously deform the oval curves to larger (smaller) size. Since the pole position is closely related to the scattering length, the curves scale roughly in accord with (14). Results for the non-local potential are qualitatively similar, so we present here only the local potential results. For the non-local potential only three channels, similar to those used in Ref. 12, were used.

In Table 1 a comparison is made between the energy level shift and width using the various methods discussed in the preceeding section for the local Yukawa potential with $\alpha = 500$ MeV. Columns 2 and 3 list the isospin 0 and 1 scattering lengths corresponding to the potential strengths $f^2/4\pi$ in the first column. The shift and width determined from (1) and the pole energy of the S matrix follow in the next two columns. When $f^2/4\pi$ is between 0.75 and 0.85 these two energies differ significantly. In this range of the potential strength, a $K^- - P$ resonance is formed near threshold (see Fig. 1), the effective range becomes large, and the approximations used in (1) are not valid. The difference between the energy found by the formula in (1) and the actual pole energy is caused by either a large effective range, as in the case considered here, or a large Coulomb correction not included in (1). A discussion of anomalous Coulomb corrections is given in Ref. 8.

Our model calculation shows that Eq. (1) is valid to within 5% for a resonance far from threshold. Consider the situation with respect to the $\Lambda(1405)$ resonance just 27 MeV below the $K^- - P$ threshold. At a value of $f^2/4\pi = 0.91$, which corresponds to a resonance at 1405 MeV, the discrepancy between the pole energy and (1) is only 10%. The width of the resonance is related to the range of the potential. The value of 500 MeV is somewhat small since it produces a width of around 35 MeV for the $\Lambda(1405)$, which is to be compared to the experimental value of 25 MeV. Similar calculations using $\alpha = 1000$ MeV (300 MeV) give 3% (16%) difference from the predictions of (1). Thus, if the $\Lambda(1405)$ is a bound state then it is probably far enough away from the $K^- - P$ threshold energy so that it does not cause any drastic modifications of (1). We note that in Ref. 12, for particular potential models which reproduce the scattering data, similar validity of (1) was found. It has been suggested that $\Lambda(1405)$ is a composite resonant state [6]. If this were the case, a similar check of (1) should be done. We have not considered this case here.

In a recent paper [16], a Coulomb-nuclear interference potential term was shown to cause substantial deviations from the predictions of (1). Here we estimated these effects by adding an interference potential in the $K^- p$ channel of the form $V_{\mathrm{Coulomb}}(r)\, V_{55}(r)$. The inclusion of this additional potential changed our results very little, $< 1\%$, since its overall strength is approximately 1/139 of V_{55}.

It is interesting to note that only a 10% increase of $f^2/4\pi$ to 1.0 gives extremely good agreement with the $K^- - P$ at rest branching ratios (see Table 2). In addition, for $f^2/4\pi$ between 0.9 and 1.0 the above

Table 2. Comparison of the $K^- - P$ at rest branching ratios γ, R_c, and R_N as calculated from the residues of the S matrix and from the threshold limit of the cross sections. Two combinations of the strength and range are presented

	Experimental value	$\frac{f^2}{4\pi}=1$; $\alpha=500$ MeV		$\frac{f^2}{4\pi}=1.44$; $\alpha=800$ MeV	
		Above threshold limit	Residue of pole	Above threshold limit	Residue of pole
γ	2.36 ±0.04 [17]	2.36	2.41	2.34	2.39
R_c	0.664±0.11 [17]	0.642	0.639	0.649	0.647
R_N	0.184±0.15 [18]	0.22	0.23	0.165	0.169

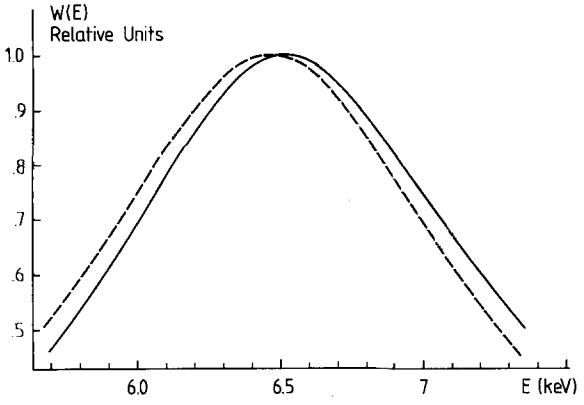

Fig. 2. Graph of the transition probability $W(E)$ (solid line) as calculated in (67) for $\alpha=500$ MeV and $f^2/4\pi=0.82$. The dotted line corresponds to a Lorentzian whose position and width are determined from the pole of the S matrix

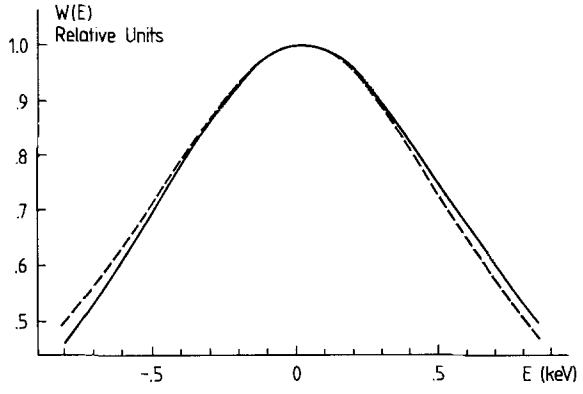

Fig. 3. Shape comparison of the transition probability $W(E)$ with a Lorentzian shape. The solid line represents $W(E)$ and the dotted line corresponds to a Lorentzian curve whose peak position and width are the same as $W(E)$

threshold scattering data are also qualitatively reproduced. These results suggest that this model is reasonable, at least with respect to the relative $SU(3)$ derived coupling strengths C_{ij}.

The peak and width of the transition probability, $W(E)$, relative to E^c_{1s} is listed in the last column. This energy is to be compared with the complex pole energy. The difference between these two values is 10–15% of Γ for $\Gamma/E_0 \simeq 0.1$. In Fig. 2 we compare the shape of the photon emission spectrum (solid line) with a Lorentzian curve corresponding to the pole energy (dashed line) for $f^2/4\pi=0.82$. Deviations are caused by a different peak energy and a different shape. For this case of large inelasticity, the difference can be substantial. Particularly if ε is small, these corrections need to be considered for determining ε reliably.

To get a feeling for the actual deviation of the spectrum from a pure Lorentzian, we have superimposed in Fig. 3 a Lorentzian shape of the same width and peak position as $W(E)$. The difference in shape is quite small except in the far tail region as seen in the figure.

As a side calculation, we compute the $K^- - P$ at rest branching ratios at threshold and at the pole energy. These are defined as

$$\gamma \equiv \frac{K^- p \to \Sigma^- \pi^+}{K^- p \to \Sigma^+ \pi^-};$$
$$R_c \equiv \frac{K^- p \to \text{Charged Particles}}{K^- p \to \text{All Final States}};$$
$$R_N \equiv \frac{K^- p \to \pi^0 \Lambda}{K^- p \to \text{All Neutral States}}. \tag{15}$$

Since the ratio γ can have a strong energy dependence, these values might have a significant variation even over this small energy range. The results are listed in Table 2 for range parameters α of 500 MeV and 800 MeV. The threshold results were calculated by taking the limit of k_5 going to zero for the above

threshold $K^- - P$ scattering cross sections including the Coulomb interaction in the $K^- - P$ channel, although neglecting this interaction had little effect on these ratios. The pole energy values were obtained by calculating the residues of the S matrix at the pole energy, and multiplying by the appropriate phase space factors. From the table it is seen that the difference is 3%.

4. Summary

A model calculation was preformed to assess the validity of the relationship between the $K^- - P$ scattering length and the X-ray spectrum of the $2p-1s$ atomic transition. Since the $K^- - P$ system has a resonance, $\Lambda(1405)$, near threshold, possible modifications of the standard relationship, Eq. (1), might be required. However, for combinations of the potential parameters which lead to a bound state resonance at 1405 MeV and reproduce widths comparable to the experimental values, only small modifications are found. The difference between the real part of the pole energy of the S-matrix and the peak of the X-ray spectrum also turned out to be small. Significant deviations result only when Γ/E_0 is of the order 0.1. In addition, this model was able to reproduce the experimental $K^- - P$ at rest branching ratios.

Thus for values of the potential parameters which reproduce approximately the experimental results with a bound state for the $\Lambda(1405)$ resonance, the relation between the scattering length and the peak and width of the X-ray spectrum is accurate at least to the order of 10%. Although a specific model has been used, the results with respect to the validity of (1) are expected to be qualitatively general. These modifications fail to resolve the disagreement of the $K^- - P$ scattering length as determined from the current low energy scattering data analysis and from the present $K^- - P$ atomic level shift data.

The author would like to thank M. Schaden, M. Kohno, W. Weise, W. Kaufmann and W. Gibbs for many useful discussions and comments on this work.

References

1. Martin, A.D.: Nucl. Phys. B **179**, 33 (1981)
2. Chao, Y.-A., Kraemar, R.W., Thomas, D.W., Martin, B.R.: Nucl. Phys. B **56**, 46 (1973)
3. Davies, J.D., et al.: Phys. Lett. **83** B, 55 (1979)
4. Izycki, M., et al.: Z. Phys. A – Atoms and Nuclei **297**, 11 (1980)
5. Bird, P., et al.: Nucl. Phys. A **404**, 482 (1983)
6. Kumar, K.S., Nogami, Y.: Phys. Rev. D **21**, 1834 (1980)
7. Deloff, A., Law, J.: Phys. Rev. C **20**, 1597 (1979); also see Kerbikov, B.O.: Sov. J. Nucl. Phys. **38**, 673 (1983); Dumbrajs, O.: Phys. Scr. **31**, 485 (1985) for Coulomb corrections to the scattering length
8. Kumar, K.S., Nogami, Y., Dijk, W. van, Kiang, D.: Z. Phys. A – Atoms and Nuclei **304**, 301 (1982)
9. Dalitz, R.H., McGinley, J., Belyea, C., Anthony, S.: p. 201; C.J. Batty, Pg. 297, "Proceedings of the International Conference on Hypernuclear and Kaon Physics" Heidelberg, Germany (1982)
10. Dalitz, R.H., Tuan, S.F.: Ann. Phys. **10**, 307 (1960)
11. Thaler, J.: J. Phys. G **10**, 1037 (1984)
12. Landau, R.H.: Phys. Rev. C **28**, 1324 (1983); Landau, R.H., Cheng, B.: Phys. Rev. C **33**, 734 (1986)
13. Thaler, J.: J. Phys. G **9**, 1009 (1983)
14. Dalitz, R.H., Wong, T.-C., Rajasekaran, G.: Phys. Rev. **153**, 1617 (1967)
15. Compilation of coupling constants and low-energy parameters. Nucl. Phys. B **216**, 277 (1983)
16. Law, J., Turner, M.J., Barrett, R.C.: Phys. Rev. C **35**, 305 (1987)
17. Tovee, D., et al.: Nucl. Phys. B **33**, 493 (1971); Nowak, R., et al.: Nucl. Phys. B **139**, 41 (1978)
18. Humphrey, W.E., Roos, R.R.: Phys. Rev. **127**, 1305 (1962); Sakitt, M., et al.: Phys. Rev. **139** B, 719 (1965); Kim, J.K.: Columbia University Report, Nevis 149 (1966)

P.B. Siegel
Institut für Theoretische Physik
Universität Regensburg
Universitätsstrasse 31
D-8400 Regensburg
Federal Republic of Germany